THERMORESPONSIVE DOUBLE NETWORK HYDROGEL MEMBRANES FOR GLUCOSE BIOSENSORS

An Honors Fellow Thesis

by

JASON THOMAS GEORGE

Submitted to Honors and Undergraduate Research
Texas A&M University
in partial fulfillment of the requirements for the designation as

HONORS UNDERGRADUATE RESEARCH FELLOW

May 2012

Major: Biomedical Engineering
Mathematics

THERMORESPONSIVE DOUBLE NETWORK HYDROGEL MEMBRANES FOR GLUCOSE BIOSENSORS

An Honors Fellow Thesis

by

JASON THOMAS GEORGE

Submitted to Honors and Undergraduate Research
Texas A&M University
in partial fulfillment of the requirements for the designation as

HONORS UNDERGRADUATE RESEARCH FELLOW

Approved by:

Research Advisor: Melissa A. Grunlan
Associate Director, Honors and Undergraduate Research: Duncan MacKenzie

May 2012

Major: Biomedical Engineering
Mathematics

ABSTRACT

Thermoresponsive Double Network Hydrogel Membranes
for Glucose Biosensors. (May 2012)

Jason Thomas George
Department of Biomedical Engineering
Texas A&M University

Research Advisor: Dr. Melissa Grunlan
Department of Biomedical Engineering

Poly(*N*-isopropylacrylamide) (PNIPAAm) hydrogels reversibly switch from a water-swollen to a deswollen state when heated above their volume phase transition temperature (VPTT = ~ 33 °C). It has been shown that PNIPAAm hydrogel surfaces release adherent cells with thermal cycling. We propose the use of PNIPAAm hydrogels as membranes for implanted biosensors to actively combat biofouling through thermal modulation. To enhance the feasibility of this approach, the hydrogel membrane must be mechanically robust, exhibit rapid swelling and deswelling properties, and operate within the temperature range of interest (~37 ºC) for protein and cell removal. Toward this goal, we have prepared PNIPAAm double network (DN) hydrogels synthesized in two steps with the first network highly crosslinked and the second loosely crosslinked in order to increase the mechanical integrity of the PNIPAAm hydrogel. Colloidal poly(dimetylsiloxane) (PDMS) nanoparticles (average diameter = ~220 nm and ~50 nm) were incorporated into the first or second network to increase swelling and deswelling kinetics. *N*-vinyl-2-pyrrolidone (NVP), a hydrophilic comonomer was introduced to

raise the VPTT above the threshold temperature. The resulting thermoresponsive nanocomposite hydrogels were characterized with respect to their morphology, mechanical properties, and swelling/deswelling behavior and release of cells upon thermal modulation. In addition, the introduction of 2-Acrylamido-2-methylpropanesulfonic acid (AMPS), a negatively charged comonomer, was explored independently in order to increase mechanical strength and improve swelling and deswelling kinetics. To utilize the hydrogel design as a functional membrane, attempts have been made to directly incorporate tetramethylrhodamine isothiocyanate concanavalin A (ConA), a glycoprotein utilized in the sensing chemistry. We investigate the delivery of ConA-loaded calcium carbonate microspheres ($CaCO_3$) into the DN hydrogels.

ACKNOWLEDGMENTS

I would like to thank my research advisor, Dr. Grunlan, for her guidance throughout my experience in undergraduate research.

I would also like to thank Rouchong Fei for countless hours of advice and guidance in addition to being an invaluable mentor.

I extend my thanks to Jeehyun Park and Kristen Means for their help with the project.

Lastly, I want to thank my family for their continued support and encouragement.

NOMENCLATURE

AMPS	2-Acrylamido-2-methylpropanesulfonic acid
BIS	*N,N′*-methylenebisacrylamide
$CaCO_3$	Calcium carbonate
ConA	Tetramethylrhodamine isothiocyanate concanavalin A
DI H_2O	Deionizied water
DMA	Dynamic mechanical analysis
DN	Double network
EDTA	Ethylenediaminetetraacetic acid
FTIC-dextran	Fluorescein isothiocyanate dextran
LCST	Lower critical solution temperature
NIPAAm	*N*-isopropylacrylamide
NVP	*N*-vinyl-2-pyrrolidone
PAMPS	Poly(2-Acrylamido-2-methylpropanesulfonic acid)
PBS	Phosphate buffered saline
PDMS	Poly(dimethylsiloxane)
PEG	Poly(ethylene glycol)
PNIPAAm	Poly(*N*-isopropylacrylamide)
SN	Single network
VPTT	Volume phase transition temperature
wt%	Weight percent

TABLE OF CONTENTS

Page

LIST OF FIGURES

LIST OF TABLES

CHAPTER I

INTRODUCTION

Diabetes

Diabetes is a metabolic disease chronically affecting over 25 million Americans and is characterized by elevated blood glucose levels. Individuals with this disease must carefully monitor their blood sugar. This is traditionally performed using an electrochemical sensor that requires a patient blood sample. Readings are accurate but glucose levels cannot be continuously monitored in this fashion, and each puncture leaves the body open to infection. Furthermore, patient compliance is low with stringent glucose monitoring.

Glucose biosensor

Continuous monitoring of blood glucose levels would allow for tighter control of diabetes. An implanted glucose biosensor would relay the information to an external display, which could then be interpreted by the user (Figure 1). In addition, the apparatus would effectively alert the patient of extreme glucose levels. Such a design for the biosensor has been conceived wherein fluorescence quenching of fluorescein isothiocyanate dextran (FTIC-dextran) by tetramethylrhodamine isothiocyanate concanavalin A (ConA) occurs when the two are bound in a poly(ethylene glycol)

This thesis follows the style of *Biomacromolecules*.

(PEG) hydrogel[1]. Liberation of FTIC-dextran via competitive binding of glucose to ConA increases fluorescence in a manner proportional to glucose concentrations.

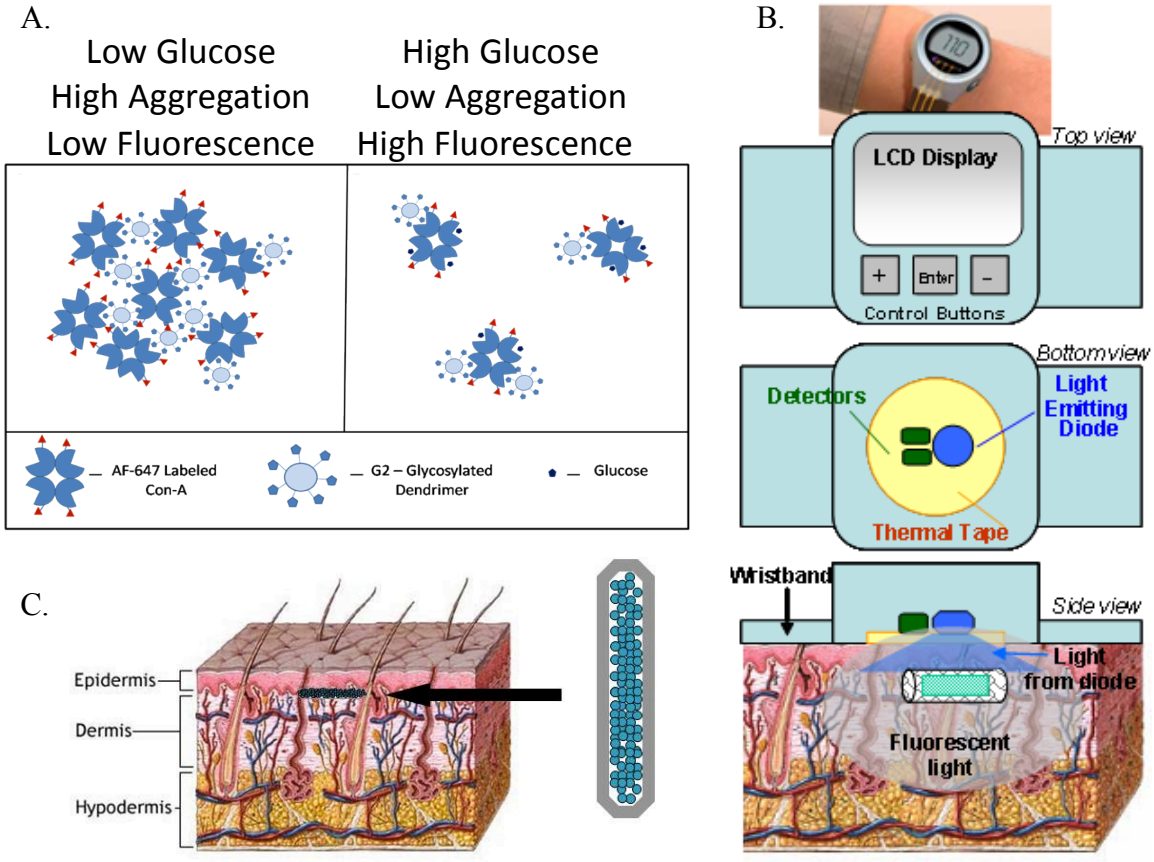

Figure 1. Glucose biosensor with sensing chemistry. (A) ConA and G2-Dendrimer sensing chemistry. (B) Schematic of biosensor readout and operation. (C) Depiction of subcutaneous implanted glucose biosensor.

Biocompatibility

Subcutaneous implantation of the sensor into the body will result in a host response to the foreign material[2]. Macrophage invasion and occlusion of the device inevitably leads

to fibrous encapsulation, hindering the ability of the biosensor to take accurate readings (Figure 2). Design of a membrane whose purpose is to prevent such a response is of central importance to device functionality. Hydrogels are a natural choice of materials as their high water content makes them biocompatible[3]. Furthermore, hydrogel design allows for variable swelling behavior dependent on external stimuli such as temperature, pH, solvent, electric and magnetic fields. Cyclic changes in swelling behavior result in reversible hydrogel collapse and reswelling that releases adherent cells.

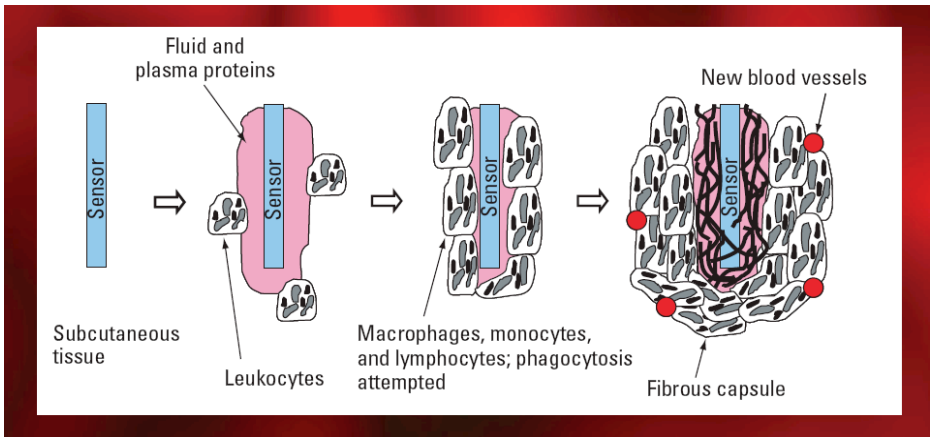

Figure 2. Membrane encapsulation. Eventual sensor encapsulation limits glucose diffusion necessary for proper readings.

NIPAAm hydrogels

Thermoresponsive hydrogels undergo this transformation with a change in temperature (Figure 3). Swelling properties are easily controlled with temperature both *in vitro* and *in vivo*. Attention has been given to a class of hydrogels fabricated from monomer with lower critical solution temperature (LCST). That is, those hydrogels which swell at low

temperatures and rapidly collapse when increased above their volume phase transition temperature (VPTT). To date, several LCST-thermoresponsive systems have been synthesized including poly(N-isopropylacrylamide) (PNIPAAm), poloxamers, xyloglucan, methylcellulose, hyroxybutyl chitosan, and human tropoelasin-like polypeptide hydrogels[4]. All but the PNIPAAm and Poloxamer systems mentioned above are derived from naturally occurring materials, which run the risk of exacerbating the host response. Further attention is directed toward the development of a PNIPAAm-based biosensor membrane.

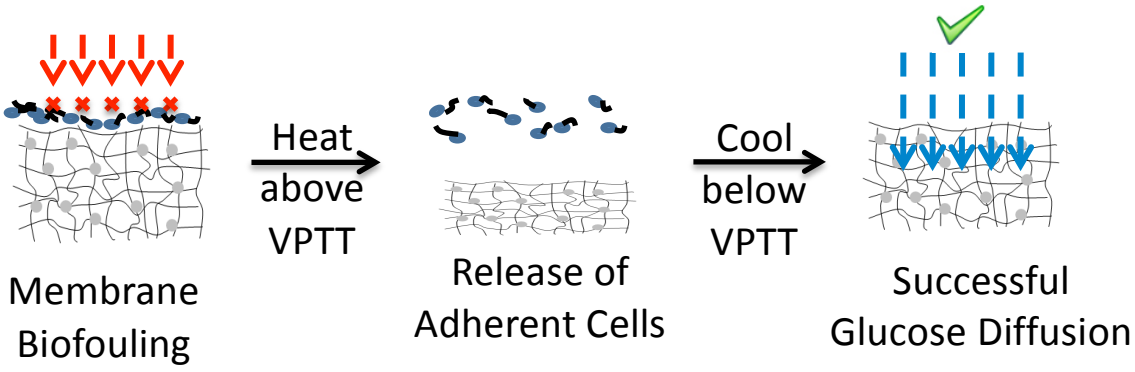

Figure 3. Membrane thermosensitivity. Thermocycling actively cleans the sensor membrane.

NIPAAm monomer contains both a hydrophobic isopropyl group and a hydrophilic amide group. Crosslinked PNIPAAm hydrogels observe a VPTT near 33°C[5]. These hydrogels transition from a hydrophilic, swollen state to a hydrophobic, deswollen state when temperatures are increased above the VPTT[6]. Because cells show greatest

adhesivity for moderately hydrophobic surfaces, PNIPAAm hydrogels provide favorable topology for cell attachment above their VPTT. Cooling below this temperature results in a hydrophilic surface which, combined with the large change in surface area, is responsible for cell detachment. It has been shown that the addition of hydrophobic polysiloxane nanoparticles increases kinetic swelling/deswelling properties f single network PNIPAAm hydrogels[7]. Hydrogel VPTT remains around 33°C with the addition of nanoparticles.

Presented research

Several improvements must be made for the successful implementation of PNIPAAm hydrogels as self-cleaning membranes *in vivo* (Figure 4). If unaltered, PNIPAAm VPTT directs the hydrogel to be fully collapsed at wrist temperature (near 35°C). This prevents thermocyclic swelling and deswelling required for cell-release. Previous designs have incorporated *N*-vinyl-2-pyrrolidone (NVP) as a co-monomer in order to raise the VPTT to physiological range[8]. It was determined that the addition of NVP significantly increased the amount of glucose diffusion through the membrane. To this point the optimal duty cycle, which would allow the most glucose diffusion while preventing cell occlusion *in vivo*, has yet to be determined. However, initial results revealed that hydrogels show very low cell adhesivity after 7 days when cycled above and below their VTPP every hour.

Additional attention has been directed toward increasing the mechanical properties of such hydrogels for *in vivo* application. One method includes implementing a double

network (DN) hydrogel design through the combination of one or more hydrophilic monomers[9]. Double network hydrogels synthesized with the electrostatic comonomer 2-Acrylamido-2-methylpropane sulfonic acid (AMPS) have displayed great increases in mechanical properties. The fracture stress of a single network gel composed of 75% AMPS relative to the total monomer concentration increases nearly 50 times with the addition of a second loosely crosslinked network. Optimal gels can withstand compressive stresses on the order of 10 MPa, which is a large improvement over gels that can be broken with a slight tug.

Double network poly(2-Acrylamido-2-methylpropane sulfonic acid) (PAMPS) hydrogels would significantly augment the biosensor membrane's mechanical properties. However, the PAMPS gels previously studied are not thermoresponsive, motivating further analysis of PNIPAAm-PAMPS gels[10]. Incorporation of AMPS with thermoresponsive NIPAAm into double-network hydrogels will be studied along with incorporation of additional components such as NVP and poly(dimethylsiloxane) (PDMS) nanoparticles in order to synthesize an optimal biosensor membrane suitable for implantation.

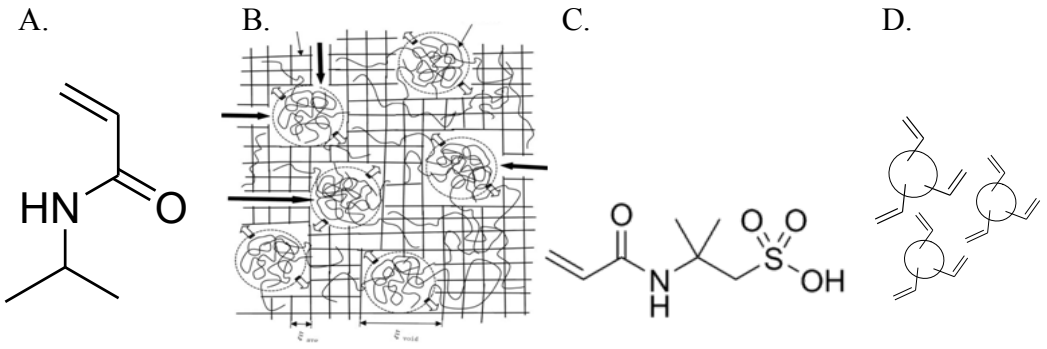

Figure 4. Key components for a functional biosensor. (A) the NIPAAm monomer provides self-cleaning properties. (B) Double network design imparts mechanical stiffness through an inhomogeneous matrix of highly crosslinked 1st network (arrows) with a 2nd, loosely crosslinked network. (C) AMPS co-monomer increases mechanical properties. (D) PDMS nanoparticles increase the swelling/deswelling properties.

A functional biosensor requires successful incorporation of ConA and dendrimer sensing chemistry into the hydrogel, and several strategies are currently being employed to achieve this end. Sensing chemistry requires space to aggregate and dissociate, which must be complimented by a sufficiently dense hydrogel network to prevent ConA leakage. ConA-loaded calcium carbonate ($CaCO_3$) microspheres will be incorporated into the precursor solution to deliver sensing chemistry directly into the hydrogel, paving the way to study the effects of crosslinking density and NIPAAm monomer concentration on ConA retention.

CHAPTER II

METHODOLOGY

Synthesis of crosslinked polysiloxane nanparticles

PDMS colloidal nanoparticles of two different average diameters (54 nm and 219 nm) were prepared by cationic emulsion polymerization as previously reported[7].

Synthesis of PDMS nanoparticle single network hydrogels

Single network (SN) hydrogels were prepared via in situ photocure of aqueous precursor solutions of 14 total weight-percent (wt%) containing NIPAAm monomer, *N,N′*-methylenebisacrylamide (BIS) crosslinker, Irgacure-2959 photoinitiator, deionized water (DI H_2O), and crosslinked polysiloxane nanoparticles (2 wt% solid nanoparticles). NIPAAm (1.0 g), BIS (0.04 g), and Irgacure (0.08 g) were dissolved in DI H_2O (7.0 g total including the volume of water introduced by nanoparticle emulsion) using a 50-mL round bottom flask equipped with a Teflon-covered stir bar. The required amount of nanoparticles was then added. Hydrogel slabs were prepared by pipetting precursor solution into a rectangular mold formed by sandwiching polycarbonate spacers (1.5 mm thick) between two clamped glass slides. The mold was submerged into an ice water bath (~7 ºC) and subjected to UV light (6 mW/cm^2, 365 nm) for 30 min. After removal from the mold, SN slabs were rinsed and then soaked in DI H_2O for 2 days with daily water changes to remove impurities.

Synthesis of PAMPS single network hydrogels

SN hydrogels were prepared via *in situ* photocure of aqueous precursor solutions containing NIPAAm monomer, AMPS monomer, BIS crosslinker, Irgacure-2959 photoinitiator, and DI H_2O. NIPAAm and AMPS monomers (total weight equal to 1.0 g), BIS (0.04 g), and Irgacure (0.08 g) were dissolved in DI H_2O (7.0 g) using a 50-mL round bottom flask equipped with a Teflon-covered stir bar. Different monomer compositions were prepared by varying the ratio of AMPS to NIPAAm (0-75 wt%). Hydrogel slabs were prepared as above.

Synthesis of double network hydrogels

The SN hydrogels were subsequently soaked in a solution of NIPAAm (6.0 g), BIS (0.012 g), Irgacure-2959 (0.24 g), and DI H_2O (21 mL) for 24 hr. Hydrogel slabs were then blotted with a Kim Wipe to remove excess solution and transferred to a rectangular mold (2.3 mm thick), photocured, and purified as above.

ConA absorbance

ConA was dissolved in phosphate buffered saline (PBS) at concentrations of 2.5, 1.25, 0.63, 0.31, 0.16, and 0.08 mg/mL. ConA absorbance was characterized by taking absorbance readings of the series at 280 nm (Ocean Optics USB4000 with 25 ms integration time, 3 scans to average) in order to determine the molar extinction coefficient.

Preparation of $CaCO_3$ containing ConA

ConA-containing $CaCO_3$ microspheres ($CaCO_3$-ConA) were prepared by adding 5 mg of ConA to a 5 mL solution of 0.33 M $CaCl_2$, and the solution was gently stirred (80 rpm) until homogeneous. The speed was increased 750 rpm and 5 mL 0.33 M Na_2CO_3 was subsequently added and mixed for 1 min. The supernatant was removed and the ConA-$CaCO_3$ spheres were then washed twice, each time with 1 mL of PBS, and lyophilized over night and refrigerated at 5 ºC (Figure 5). The resulting supernatant and wash was then analyzed to determine loading efficiency by measuring the amount of ConA left in solution.

Figure 5. Lyophilized ConA-containing $CaCO_3$ microspheres

Preparation of $CaCO_3$-ConA single network hydrogels

$CaCO_3$-ConA containing hydrogels were prepared by *in situ* photocure of aqueous precursor solutions as above for the PAMPS SN hydrogels (Figure 6). In a 500mL round bottom flask equipped with a Teflon-covered stir bar, NIPAAm (1.0 g), BIS (0.04 g), Irgacure (0.08 g), PDMS nanoparticles (2 wt% solid nanoparticles based on NIPAAm weight), and NVP comonomer (2 wt%) were dissolved in PBS (7.0 g). Slab sheets were prepared by pipetting precursor solution between two clamped glass microscope slides separated by polycarbonate spacers (1.5 mm thick), and cylindrical hydrogels were fabricated by inserting precursor solution into a glass annulus (inner diameter 1 mm). The mold was submerged in an ice water bath (~7 ºC) and exposed to UV light (6 mW/cm^2, 365 nm) for 30 min. After removal from the mold, the hydrogel sheet was rinsed and soaked in PBS for 1 day with 2 replacements to remove impurities.

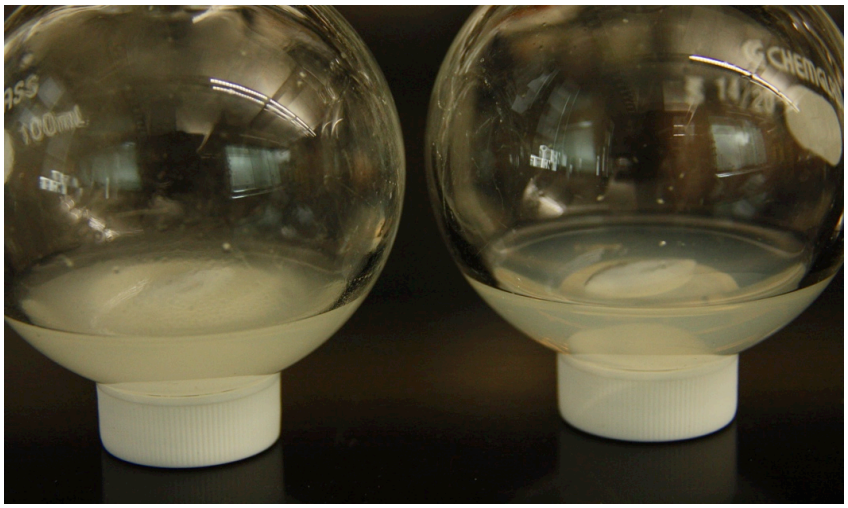

Figure 6. Membrane precursor solutions. (Left) Precursor solution containing $CaCO_3$-ConA microspheres. (Right) Precursor solution without microspheres.

Preparation of $CaCO_3$-ConA double network hydrogels

$CaCO_3$-ConA SN hydrogels were subsequently soaked in a solution of NIPAAm (6.0 g), BIS (0.012 g), Irgacure-2959 (0.24 g), and PBS (21 mL) for 24 hr. Hydrogels were blotted with a Kim wipe to remove excess solution. Slabs were transferred to a rectangular mold (2.3 mm thick) and cylindrical hydrogels were transferred to a glass annulus (inner diameter 3 mm). The gels were then similarly photocured at 7 ºC and soaked in PBS for 2 days with daily water changes prior to analysis (Figure 7).

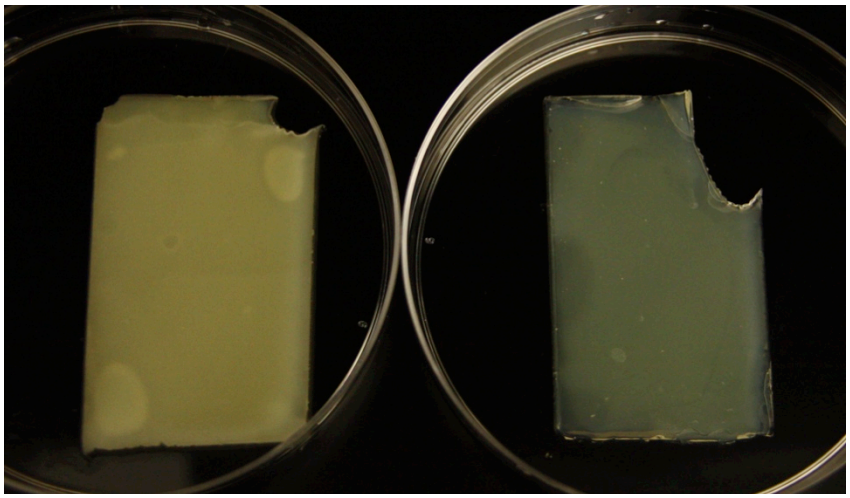

Figure 7. Double network hydrogels. (Left) DN hydrogel containing $CaCO_3$-ConA microspheres; (Right) DN hydrogel without microspheres.

Removal of incorporated $CaCO_3$

In order to provide the sensing chemistry with sufficient space to function, $CaCO_3$-ConA-loaded DN hydrogels were soaked in a solution of 0.05 M Ethylenediaminetetraacetic acid (EDTA) dissolved in DI H_2O for 2 hr with 1 replacement after the first hour (Figure 8).

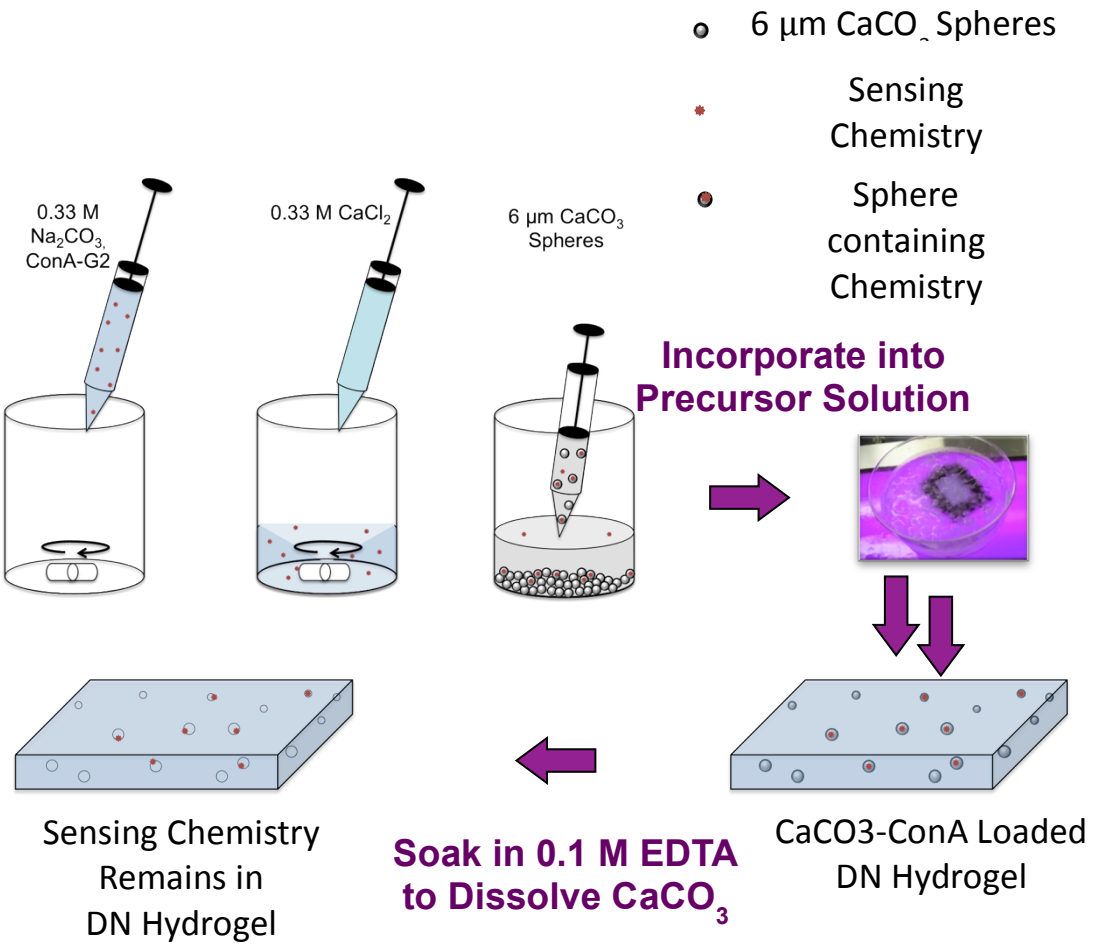

Figure 8. $CaCO_3$-loaded hydrogel synthesis. Loaded $CaCO_3$ spheres are incorporated directly into the hydrogel slab, and then subsequently dissolved out to leave sensing chemistry behind.

Morphology

$CaCO_3$-ConA DN hydrogels washed with 0.05 M EDTA were immersed in liquid nitrogen and subsequently freeze-dried in a lyophilizer overnight. Cross sections were platinum sputter-coated and viewed under a field emission scanning electron microscope with an accelerated electron energy of 10 keV.

Volume phase transition temperature

The VPTT of slab hydrogels was determined by Differential Scanning Calorimetry (DSC, TA Instruments Q100). Swollen Hydrogels were blotted with a Kim Wipe, sealed in a hermetic pan, cooled to -50 ºC, and subsequently heated to 50 ºC at a rate of 3 ºC per min for 2 cycles. Reported data is the 2nd cycle.

Dynamic mechanical analysis (DMA)

Five swollen hydrogel discs (13 mm diameter) were punched from a single hydrogel slab with a die. DMA of the discs was measured in compression mode using a parallel-plate compression clamp with a diameter of 40 mm (bottom) and 15 mm (top). Discs were blotted with a Kim Wipe and clamped between plates with silicone oil placed around the exposed hydrogel edge to prevent water loss. Specimens were individually tested in a multi-frequency strain mode (1-25 Hz) following equilibration below the VPTT at 25 ºC for 5 min.

Kinetic deswelling

Three hydrogel discs (13 mm diameter) were prepared as above and placed in a sealed vial containing 20 mL DI H_2O, immersed in a 22 ºC water bath for 24 hr to reach equilibrium (W_s), then immediately transferred to a 50 ºC water bath. Discs were removed at 10, 20, 40, 80, 120, and 180 min, blotted with a Kim Wipe, weighed (W_t), and returned to the vial. Afterward, discs were dried in a vacuum oven (30 in. Hg, 60 ºC, 24 hr) and weighed (W_d). Water retention was defined as $WR = (W_t - W_d)/W_s$.

Kinetic reswelling

Three hydrogel discs (13 mm diameter) were prepared as above, placed in an opened vial, dried in a vacuum oven (30 in. Hg, 60 ºC, 24 hr), and weighed (W_d). 20 mL DI H_2O was added to each vial before being sealed an immersed in a water bath at 22 ºC. Discs were removed at 10, 20, 40, 80, 120, 200, 320, 450, and 640 min, blotted with a Kim Wipe, weighed (W_t), and returned to the vial. Swelling ratio was defined as $WR=W_t/W_d$.

CHAPTER III

RESULTS AND DISCUSSION

Table 1: Notation of hydrogel abbreviations*

Notation	1st network % Nanoparticles	2nd network % Nanoparticles	1st network Relative % AMPS	1st network Relative % NIPAAm
SN	--	(No 2nd Network)	--	100
DN	--	--	--	100
200-1	2 (200 nm)	--	--	100
200-2	--	2 (200 nm)	--	100
50-1	2 (50 nm)	--	--	100
50-2	--	2 (50 nm)	--	100
N%	--	--	N	100-N

*N represents the relative percentage of AMPS in the first network of PAMPS DN hydrogels.

Double network hydrogel morphology

SEM images of hydrogels are depicted below using the notation in Table 1 (Figure 9). Hydrogel morphology varies greatly with composition. The 200-1 DN hydrogels have much larger pores likely caused by a high concentration of large PDMS nanoparticles in the first network. This is expected to result in improved hydrogel swelling behavior. Pore size also increases in the PAMPS-containing DN hydrogels.

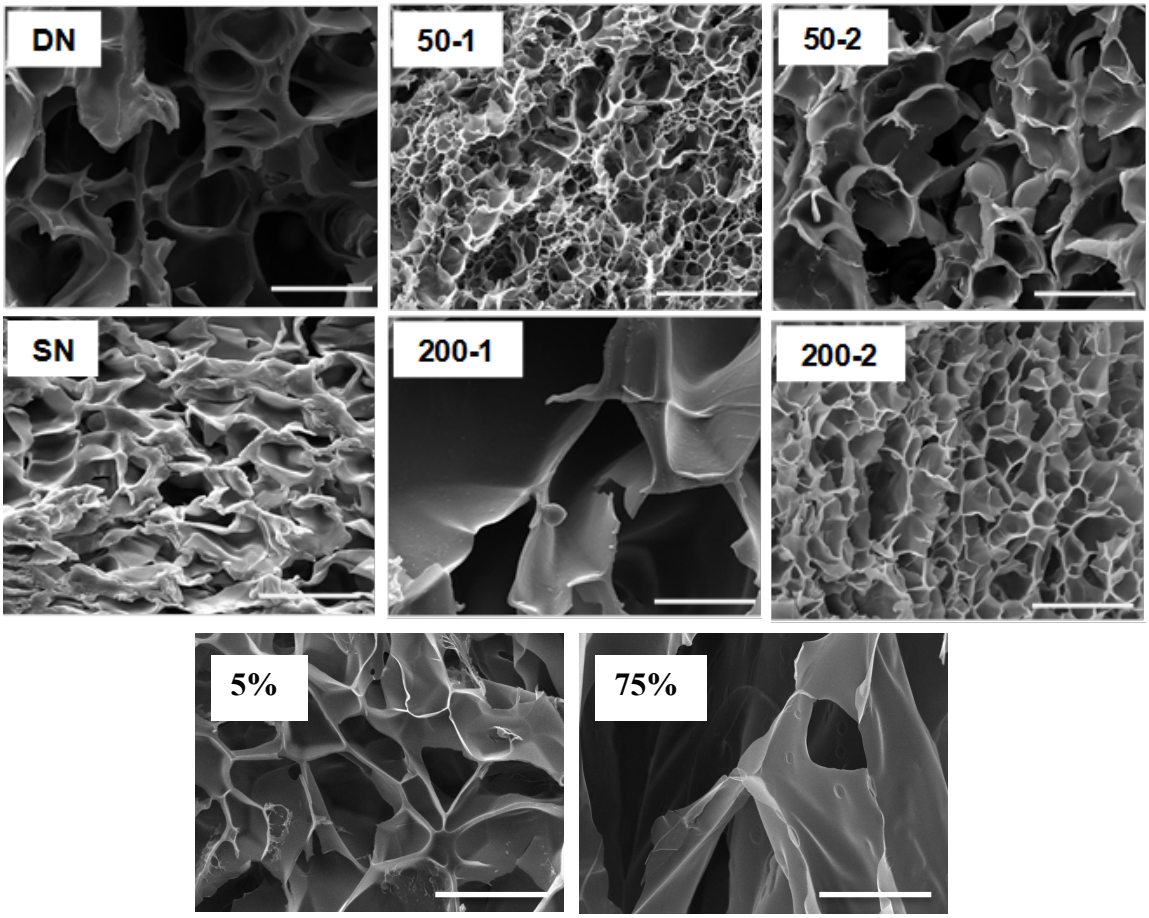

Figure 9. Double network hydrogel morphology. SEM micrograph images of DN hydrogels. All scale bars = 20 μm.

Kinetic swelling/deswelling

A functional biosensor requires a rapid change in water content in order to cause the drastic change in membrane surface area required for cell detachment, and such a change is indicated by swelling and deswelling kinetics. Deswelling properties of PDMS and PAMPS DN hydrogels are shown below in Figures 10 and 11. The addition of either nanoparticles or AMPS comonomer in the first network significantly increases the rate at which the DN hydrogel releases water. The swelling ratio of 200-1 hydrogels stands out and is attributed to their large pore size.

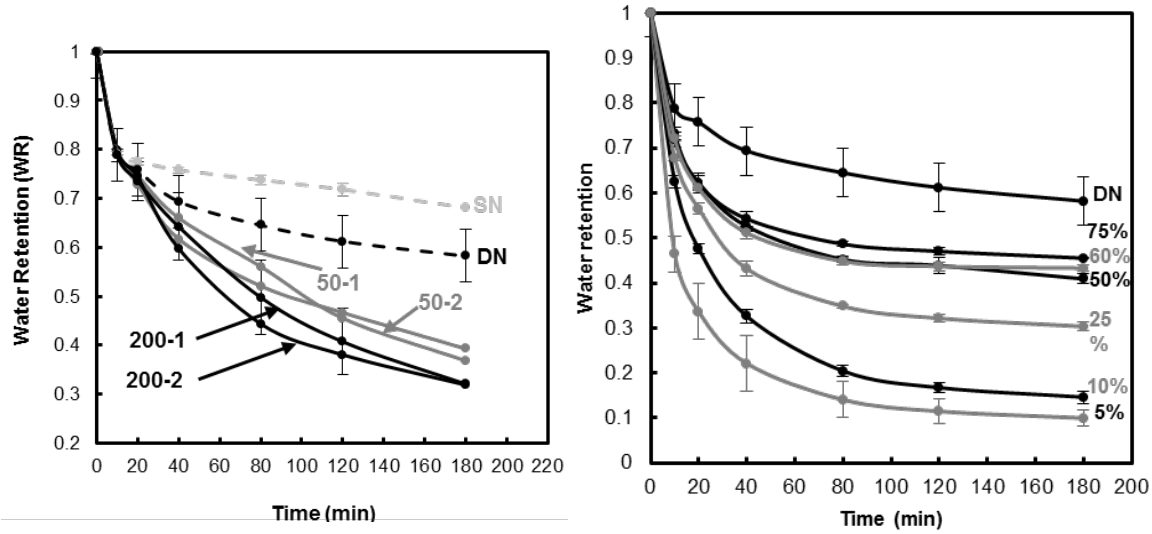

Figure 10. Hydrogel deswelling kinetics. Hydrogel deswelling kinetics at 50 ºC of (Left) PDMS DN hydrogels and (Right) PAMPS DN hydrogels.

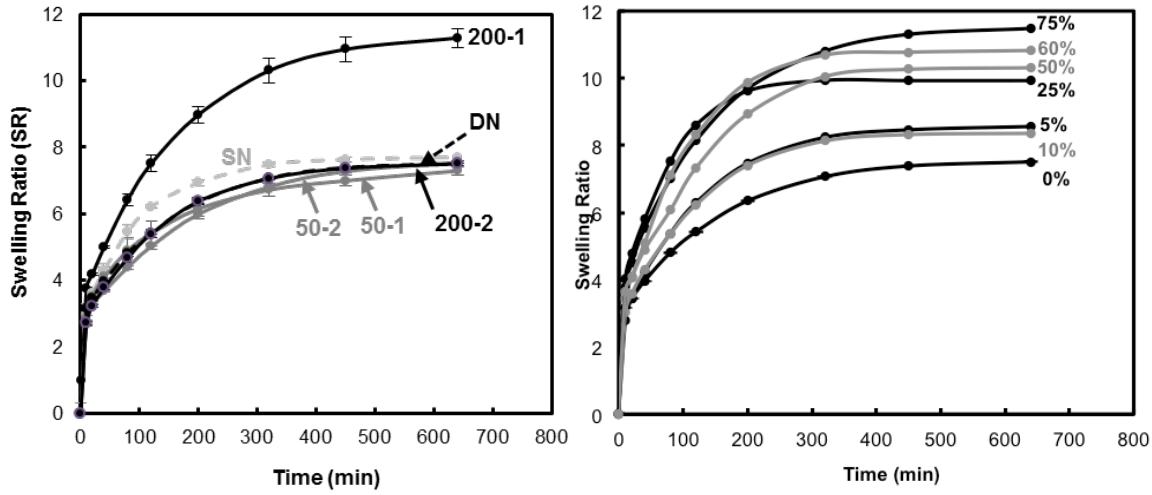

Figure 11. Hydrogel reswelling kinetics. Hydrogel reswelling kinetics at 22 ºC of (Left) PDMS DN hydrogels and (Right) PAMPS DN hydrogels.

Dynamic mechanical analysis

Hydrogel stiffness was characterized by the storage modulus, G′, given as a function of frequency of applied compressional strain (Figure 12). PDMS containing hydrogels have a diminished ability to elastically resist deformation, particularly when nanoparticles are present in the first network. Hydrogel stiffness increases initially with added AMPS, then decreases when the NIPAAm composition of the first network falls below 50%, seen in samples containing 60% and 75% AMPS. Electrostatic repulsion between neighboring chains in the first network stiffens the hydrogel but also increases water sequestration, consistent with the kinetic swelling data. This results in a decrease in stiffness of the 60% and 75% compositions.

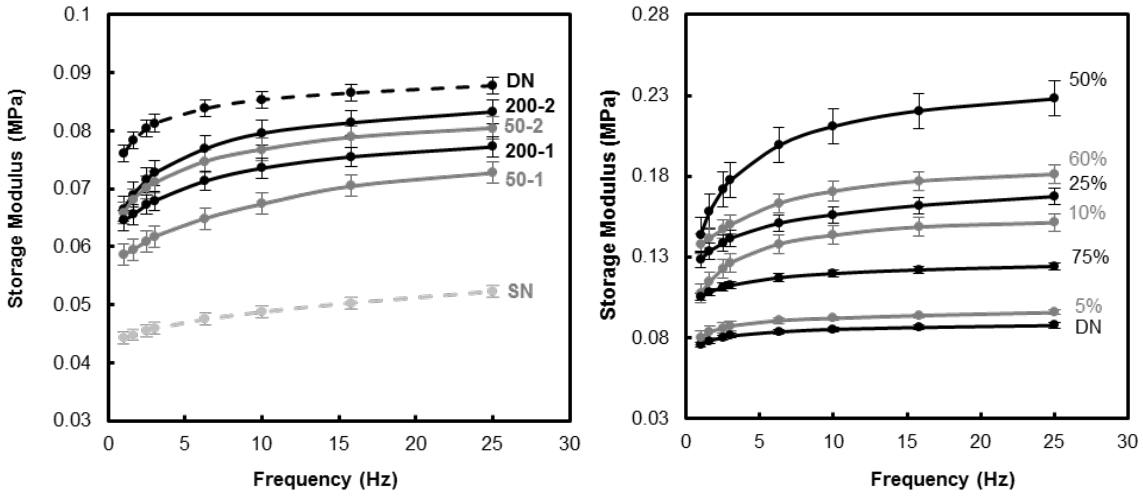

Figure 12. Dynamic mechanical analysis. DMA tests of (Left) PDMS DN hydrogels and (Right) PAMPS DN Hydrogels.

Volume phase transition temperature

The VPTT of DN hydrogels containing PDMS nanoparticles or AMPS relative to the respective SN and DN hydrogels is illustrated in Figure 13. The addition of nanoparticles in either the first or second network does not alter the VPTT. The VPTT of PAMPS hydrogels was 2-3 ºC lower in comparison to the pure PNIPAAm DN hydrogel, which would prove problematic in the development of a self-cleaning membrane. However, incremental addition of NVP comonomer raises the VPTT of the PNIPAAm DN hydrogel. It is therefore advantageous to optimize the hydrogel membrane's mechanical and swelling/deswelling properties before tuning the VPTT for a functional sensor *in vivo.*

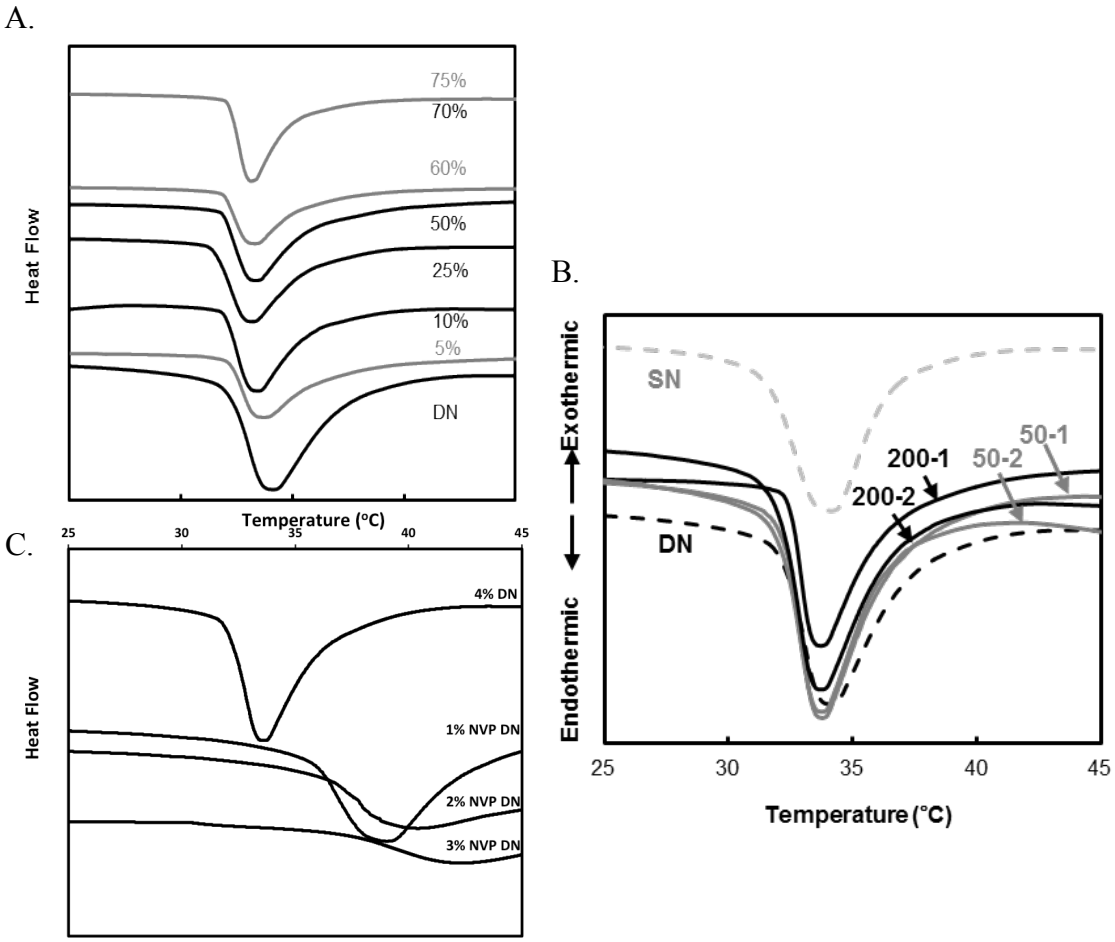

Figure 13. Volume phase transition temperature. (A) DN PAMPS hydrogels compared to pure PNIPAAm DN. (B) PDMS-containing hydrogels compared to pure DN and pure SN. (C) the addition of NVP increases the VPTT of the pure PNIPAAm DN.

ConA absorbance

The molar extinction coefficient for ConA absorbance at 280 nm (Figure 14) was determined experimentally using least squares linear regression to be

$0.872 \cdot 10^5$ L mol^{-1} cm^{-1} (0.838 mL $mg^{-1}cm^{-1}$) with a correlation coefficient of R=0.996. The molar extinction coefficient was used to measure the weight of loaded ConA during $CaCO_3$ microsphere synthesis.

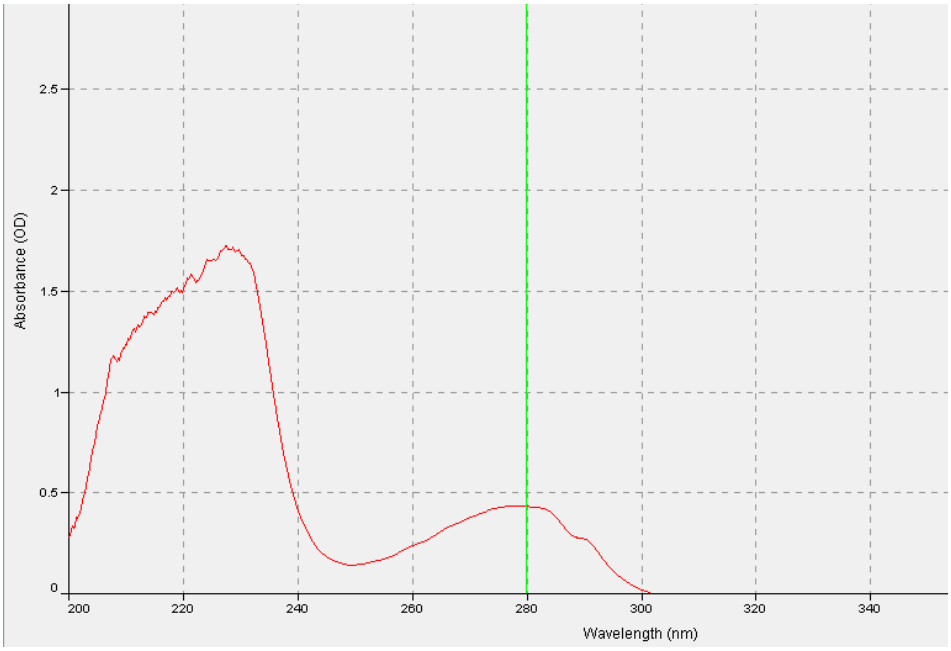

Figure 14. ConA absorbance spectra. Absorbance spectra of 2.5 mg/mL ConA in 0.05 M EDTA.

$CaCO_3$-ConA loading

Measuring ConA absorbance in the supernatant revealed a loading efficiency of 27% ± 7%, providing an estimate for later work with fluorescent ConA. These results will be used as a benchmark for further tests that aim to improve loading efficiency. Attempts to directly confirm loading efficiency using UV absorbance have been problematic due

to dissolved $CaCO_3$ and unreacted hydrogel impurities that also absorb at 280 nm. An atypical absorbance spectra is illustrated in Figure 15.

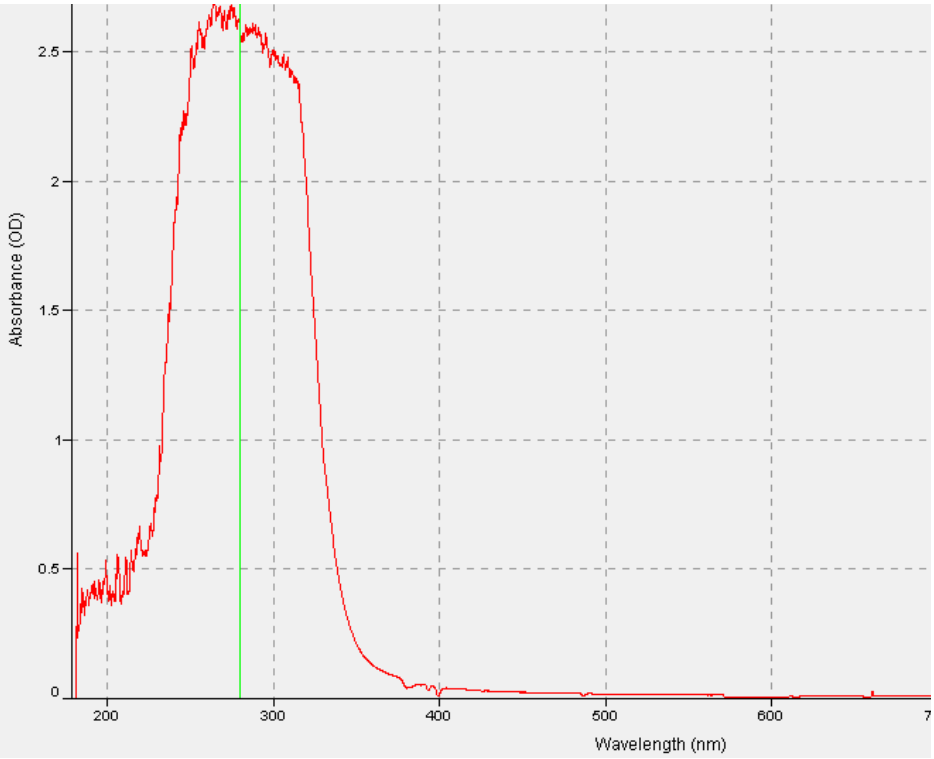

Figure 15. $CaCO_3$-ConA hydrogel EDTA wash absorbance spectra.

$CaCO_3$-ConA hydrogel morphology

SEM images of $CaCO_3$-ConA hydrogels are depicted below (Figure 16). The presence of $CaCO_3$ microspheres in the walls of the hydrogel matrix is significantly less evident in the sample treated with 0.05 M EDTA. This indicates that the microspheres have been dissolved, leaving ConA encapsulated in the newly formed pores.

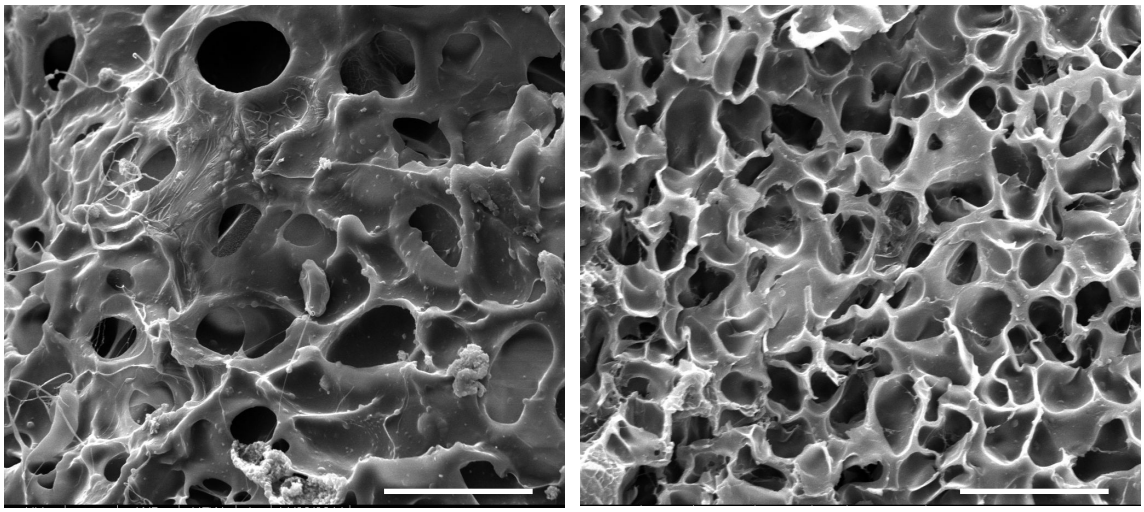

Figure 16. $CaCO_3$-ConA double network hydrogel morphology. (Left) SEM micrograph of 200-1 hydrogel containing $CaCO_3$-ConA. (Right) micrograph of 200-1 hydrogel containing $CaCO_3$-ConA and washed with 0.05 M EDTA. Scale bars = 20 μm.

CHAPTER IV

CONCLUSION

Membrane tunability

DN PNIPAAm hydrogels are a promising choice for use as a self-cleaning membrane for glucose biosensors due to their favorable thermoresponsive and mechanical properties. The addition of 200 nm PDMS nanoparticles in the first network significantly improves swelling and deswelling behavior in the gels at the cost of reducing the storage modulus, consistent with the observation of a large porous network. The AMPS comonomer effectively doubles the storage modulus of the pure PNIPAAm DN hydrogel as well as improves swelling and deswelling kinetics.

Membrane VPTT is an important consideration for *in vivo* self-cleaning applications. With a VPTT significantly lower than the body temperature at the implantation site (~37 ºC), the membrane will be in a permanently collapsed state. While PDMS nanoparticle addition does not change VPTT, AMPS decreases the VPTT by several degrees. Fortunately, the addition NVP comonomer raises the VPTT by an amount proportional to NVP concentration. In this way, a final hydrogel design can be tuned with NVP in order to ensure the proper VPTT.

$CaCO_3$-ConA studies and future work

Direct incorporation of sensing chemistry into the hydrogel by $CaCO_3$-encapsulated ConA offers a convenient delivery method as EDTA dissolving of $CaCO_3$ creates pores required for sensing chemistry aggregation and dissociation. EDTA was determined to be effective at low concentrations without ConA's denaturation, and the loading efficiency provide a context for how much chemistry is being delivered to the gel. Future studies shall include incorporate altering the total NIPAAm wt% in an attempt to minimize chemistry leakage, and measuring the fluorescent signal as a function of glucose concentration.

REFERENCES

(1) Russel, R. J.; Pishco, M. V.; Gefrides, C.C.; McShane, M.J.; Cotè, G.L. A fluorescence-based glucose biosensor using concanavalin A and dextran encapsulated in a poly(ethylene glycol) hydrogel. *Anal. Chem.* **1999**, *71*, 3126-3132.

(2) Morais, J.M. Biomaterials/tissue interactions: possible solutions to overcome foreign body response. *AAPS* **2010** *12*, 188-196.

(3) Kopeček, J.; Yang, J. Review Hydrogels as smart biomaterials. *Polym. Int.* **2007**, *56*, 1078-1098.

(4) Andriola, A.K.; Brun-Graeppi, S.; Richard, C.; Bessodes, M.; Scherman, D.; Merten, O-W. Thermoresponsive surfaces for cell culture and enzyme-free cell detachment. *Prog. Polym. Sci.* **2010**, *35*, 1311-1324.

(5) Hirokawa, Y.; Tanaka, T.; Volume phase transition in a nonionic gel. *J. Chem. Phys.* **1984**, *81*, 9379–9380.

(6) Okano, T.; Kikuchi, A.; Sakurai, Y.; Takei, Y.; Ogata, N. Temperature-responsive poly(N-isopropylacrylamide) as a modulator for alteration of hydrophilic/hydrophobic surface properties to control activation/inactivation of platelet. *J Control Release* **1995**, *36*, 125–133.

(7) Hou, Y.; Matthews, A.; Smitherman, A. M.; Bulick, A. S.; Hahn, M. S.; Hou, H.; Han, M. S.; Grunlan, M. A. Thermoresponsive nanocomposite hydrogels with cell-releasing behavior. *Biomaterials* **2008**, *29*, 3175-3184.

(8) Gant, R. M.; Abraham, A. A.; Hou, Y.; Cummins, B. M.; Grunlan, M. A.; Coté, G. L. Design of a self-cleaning thermoresponsive nanocomposite hydrogel membrane for implantable biosensors. *Acta Biomaterialia* **2010**, *6*, 2903-2910.

(9) Gong, J.P.; Katsuyama, Y.; Kurokawa, T.; Osada, Y. Double-Network Hydrogels with Extremely High Mechanical Strength. *Adv. Mater.* **2003**, *15*, 1155-1158.

(10) Fei, R.; George, J.T.; Park, J.; Grunlan, M.A. Thermoresponsive nanocomposite double network hydrogels. *Soft Matter* **2011**, *8*, 481-487.

CONTACT INFORMATION

Name:	Jason Thomas George
Professional Address:	c/o Dr. Melissa A. Grunlan Department of Biomedical Engineering 5030 Emerging Technologies Building 3120 TAMU Texas A&M University College Station, TX 77843
Email Address:	jason.g89@gmail.com
Education:	B.S., Biomed. Eng., Texas A&M University, May 2012 B.A., Mathematics, Texas A&M University, May 2012 Summa Cum Laude Undergraduate Research Fellow Alpha Eta Mu Beta